JOURNAL OF GEOPHYSICAL RESEARCH, VOL. 114, XXXXXX, doi:10.1029/2008JG000910, 2009

Scaling up ecohydrological processes: Role of surface water flow in water-limited landscapes

Alexander Popp,[1] Melanie Vogel,[2] Niels Blaum,[3] and Florian Jeltsch[3]

Received 11 December 2008; revised 16 July 2009; accepted 4 August 2009; published XX Month 2009.

[1] In this study, we present a stochastic landscape modeling approach that has the power to transfer and integrate existing information on vegetation dynamics and hydrological processes from the small scale to the landscape scale. To include microscale processes like ecohydrological feedback mechanisms and spatial exchange like surface water flow, we derive transition probabilities from a fine-scale simulation model. We applied two versions of the landscape model, one that includes and one that disregards spatial exchange of water to the situation of a sustainably used research farm and communally used and degraded rangeland in semiarid Namibia. Our simulation experiments show that including spatial exchange of overland flow among vegetation patches into our model is a precondition to reproduce vegetation dynamics, composition, and productivity, as well as hydrological processes at the landscape scale. In the model version that includes spatial exchange of water, biomass production at light grazing intensities increases 2.24-fold compared to the model without overland flow. In contrast, overgrazing destabilizes positive feedbacks through vegetation and hydrology and decreases the number of hydrological sinks in the model with overland flow. The buffer capacity of these hydrological sinks disappears and runoff increases. Here, both models predicted runoff losses from the system and artificial droughts occurring even in years with good precipitation. Overall, our study reveals that a thorough understanding of overland flow is an important precondition for improving the management of semiarid and arid rangelands with distinct topography.

Citation: Popp, A., M. Vogel, N. Blaum, and F. Jeltsch (2009), Scaling up ecohydrological processes: Role of surface water flow in water-limited landscapes, *J. Geophys. Res.*, *114*, XXXXXX, doi:10.1029/2008JG000910.

1. Introduction

[2] Decisions for the conservation of biodiversity and sustainable management of natural resources are made for long time periods and at broad spatial scales [*Peters et al.*, 1997; *Miller et al.*, 2004]. In contrast, our understanding of the underlying ecological processes (e.g., local water availability triggering germination rates and plant growth) is high at fine spatial and temporal scales because most empirical data are collected for small areas and over a short duration only [*Levin*, 1992; *Rastetter et al.*, 2003]. Therefore, the knowledge from short-term and fine-scale studies needs to be projected to regional and global scales that are relevant for decision making [*Wessman*, 1992].

[3] However, extrapolation of information across scales provides difficulties as we do not know to which extent spatial exchange, like the movement of surface water by run-off in water limited environments, affects ecosystem dynamics at large scales [*Levin*, 1992; *Tongway and Ludwig*, 1997; *Wootton*, 2001; *Strayer et al.*, 2003; *Urban*, 2005]. Omission of these processes may directly affect the accuracy of predictions [*Heuvelink*, 1998, *Weaver and Perera*, 2004]. Run-off occurs at multiple spatial scales if rainfall intensity exceeds soil infiltration capacity [*Rango et al.*, 2006]. Local differences in infiltration capacity are induced by topography, soil texture and positive feedback mechanisms between water and vegetation [*Wilcox et al.*, 2003].

[4] Many arid landscapes are source sink systems, where plant productivity is determined by surface run-off from bare areas to vegetated patches. Therefore, theoretical [*Noy-Meir*, 1973; *Scheffer et al.*, 2001; *Ludwig et al.*, 2005; *Urban*, 2005; *Peters and Havstad*, 2006] and model investigations [*van de Koppel et al.*, 2002; *van de Koppel and Rietkerk*, 2004] suggest that spatial redistribution of rainfall by run-off increases the productivity and resilience of arid ecosystems.

[5] Disturbances like unsustainable grazing can disrupt this fundamental process by changing vegetation structure and composition [e.g., *Ludwig et al.*, 2005]. The system may lose its buffer capacity and become less efficient at trapping run-off, leading to a loss of water. Today, some 20–30% of global drylands [*Winand Staring Centre*, 1991; *Reid*, 2005; *Zika and Erb*, 2009] and 30% of drylands in

[1]Potsdam Institute for Climate Impact Research, Potsdam, Germany.
[2]Natural Resources and the Environment Division, Council for Scientific and Industrial Research, Pretoria, South Africa.
[3]Department of Plant Ecology and Nature Conservation, University of Potsdam, Potsdam, Germany.

0148-0227/09/2008JG000910$09.00

Sub-Sahara Africa [*Zika and Erb*, 2009] are already degraded. Maintaining so-called 'resource conserving' dry lands [*Wilcox et al.*, 2003] will have profound implications for management of semiarid and arid rangelands especially in the future if climate change will likely lead to a general decrease in the grass resource, increase dryland vulnerability to degradation and add an additional pressure on these systems already prone to degradation.

[6] In the past, spatial transition based models like Markov chains have often been used to explore vegetation dynamics over long time periods and on large scales [e.g., *Baker*, 1989; *Turner*, 1989; *Acevedo et al.*, 1995; *Balzter*, 2000; *Logofet and Lesnaya*, 2000; *Urban*, 2005]. They are based on stochastic processes and can be parameterized by estimating transition probabilities between discrete states of the observed system. Most previous studies utilized data sampled from field surveys, existing maps, aerial photographs or satellite images to estimate transition probabilities [e.g., *Muller and Middleton*, 1994; *Brown et al.*, 2000; *Jenerette and Wu*, 2001; *Weng*, 2002], and only very few studies exist that make use of a fine-scale model to drive a landscape model [e.g., *Acevedo et al.*, 1995]. Generally, uncertainty in these studies remains relatively high because spatial exchange data such as surface water run-off are not considered. Furthermore, as very few studies do exist that describe processes at the landscape scale mechanistically [e.g., *Acevedo et al.*, 1995], data is limited and transition probabilities are often derived from short-term data [*Baker*, 1989; *Urban*, 2005].

[7] In this study we developed a method to transfer and integrate existing information on vegetation dynamics and hydrological processes in arid rangelands between spatial scales. We used a small-scale simulation model [*Popp et al.*, 2009], that was developed to investigate the relative impact of small-scale soil-plant interactions on vegetation dynamics at the hillslope scale, to derive transition probabilities between different vegetation states, productivity coefficients of different vegetation types, and hydrological parameters for a model operating at the landscape scale. We applied this modeling approach on a dwarf shrub savannah with distinct topography in arid southern Namibia to assess the role of surface water flow at the landscape scale for low and high grazing intensities.

2. Material and Methods

[8] Two variants of a stochastic and spatially explicit landscape model were implemented on the basis of Markovian modeling that simulates annual biomass production of a dwarf shrub savannah with distinct topography in arid southern Namibia (Karas Region). One version simulates lateral exchange of surface water, whereas explicit consideration of overland flow is eliminated in the second version. We used a small-scale simulation model (Topographical Management (TOPMAN)) [*Popp et al.*, 2009], that was developed to investigate the relative impact of small-scale soil-plant interactions on vegetation dynamics at the hillslope scale, to derive data which is handed over to the landscape model. This mechanistic approach guarantees that data collected and processes estimated at smaller scales are included in our application. Elevation of the landscape's grid cells was parameterized by remotely sensed digital elevation models (DEM). We computed annual productivity of the four most abundant vegetation types for two contrasting land management systems: a sustainably used research farm (for Karakul sheep breeding) and communal farming land, on which livestock grazing pressure is not controlled.

2.1. Study Area

[9] The study area is located in the Nama Karoo, southern Namibia (Figure 1). Vegetation cover and productivity are low and depend on erratic and highly variable rainfall (annual mean: 150 mm). The main topographical features of the study area are flat regions, as well as regions with gentle and precipitous slopes [*Kuiper and Meadows*, 2002]. Perennial grasses (e.g., *Stipagrostis uniplumis*) dominate the herbaceous vegetation if the rangeland is in good condition but are replaced by annual grasses (such as *Schmidtia kalahariensis*) and unpalatable shrubs (like *Rhigozum trichotomum*) when rangeland is heavily utilized [*Kuiper and Meadows*, 2002]. The most important land use in the communal area (Nabaos) and the Research Station (Gellap Ost) is small stock farming. Gellap Ost has 160 purposely understocked camps (0.05 SSU – small stock unit ha^{-1}), where animals graze in a rotational system. Resting periods of camps (no grazing) of at least one year prevent overgrazing [*Kuiper and Meadows*, 2002]. In contrast, Nabaos is managed under a communal land tenure system where livestock movement in the area is not controlled and overstocking (0.2 SSU ha^{-1}) has a strong impact on the rangeland resource.

2.2. Landscape Model

[10] The grid based landscape model simulates vegetation dynamics and interlinked hydrological processes of a dwarf shrub savannah with distinct topography in arid southern Namibia. Data on these dynamics and processes are derived from a small-scale (spatial resolution: 3×3m cells, 33×33 cells ≈ 1 ha) and spatially explicit simulation model (TOPMAN) [*Popp et al.*, 2009]. The area simulated by the small-scale model (1 ha) was used as the spatial resolution (cell size) for the landscape model. Each cell is specified by its position within the grid, elevation, productivity, vegetation composition and water availability (composed of precipitation and surface run-off). Generally, water availability is composed of the interplay of precipitation, overland flow, deep percolation and total evapotranspiration, which is composed of vegetation interception, evaporation from the soil and transpiration by plants [*Wilcox et al.*, 2003]. However, the landscape model does not consider all of these processes explicitly: Recent research suggests that deep drainage and groundwater recharge do not occur in many arid and semiarid landscapes. This is mainly because the potential for increased deep percolation during wet years is countered by an increase in the density of plants, a concomitant increase in the density of deep roots, and possibly an increase in the depth of the root zone as well [e.g., *Walvoord et al.*, 2002; *Seyfried et al.*, 2005]. Second, we disregarded vegetation interception because, in contrast to humid landscapes [e.g., *Crockford and Richardson*, 2000], vegetation cover in arid and semiarid regions has comparatively little effect on vegetation interception in arid environments [*Huxman et al.*, 2005]. Third, we did not

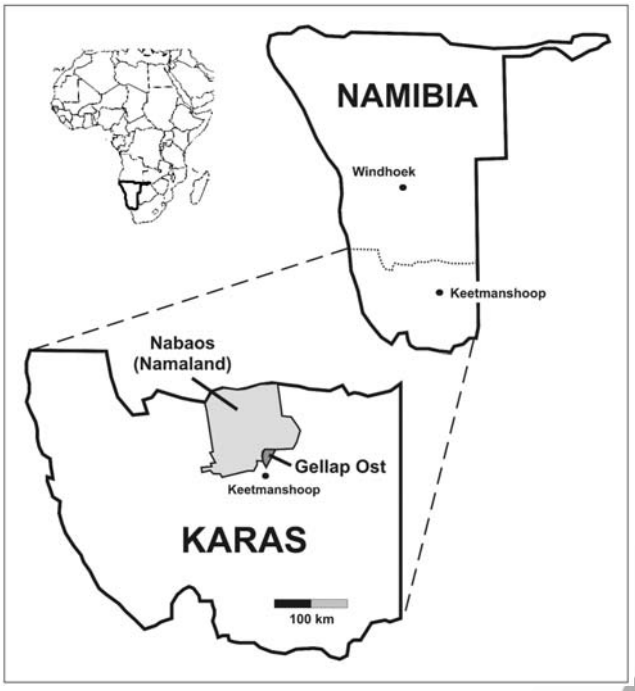

Figure 1. Location of the two case studies commercial research farm Gellap Ost and communal rangeland Nabaos.

include small-scale soil-plant interactions that affect infiltration and evaporation from the soil because these processes are already brought in via the small-scale model [see *Popp et al.*, 2009].

[11] Dynamics of the simulated vegetation types (perennial grass, annual forbs, dwarf shrubs and shrubs) on the cell level are based on the concept of state and transition models [*Westoby et al.*, 1989]. These models provide a relatively simple, management-oriented way to classify land condition (state) and to analyze the impact of factors that might cause a shift to another state (transition). The stochastic process of state and transition models and resulting forecasting of land cover change can be projected by Markov chain models [*Markov*, 1907]. To construct a Markov chain, we first identified vegetation states for the research area jointly with Namibian rangeland experts (including farmers and extension officers). The definition of these six states is related to the percentage cover of shrubs and perennial grasses (Table 1).

[12] Subsequently, we calculated annual transition probabilities between these states from simulations using TOPMAN [*Popp et al.*, 2009] for different classes of slope, rainfall and land use. For slope, we defined four classes: flat (<6%), gentle (6–10%), steep (11–15%) and precipitous (>15%). Water availability was classified in four categories, relative to the long-term mean of 150 mm: 1 is poor (<100 mm), 2 is moderate (100–139 mm), 3 is good (140–179 mm), and 4 is very good (>180 mm). Finally, we defined three categories of land use: no grazing, understocked grazing (0.05 small stock unit (SSU) ha^{-1}) and overstocked (0.2 SSU ha^{-1}) grazing. In contrast to the communal and 'overstocked' land tenure system at Nabaos where livestock movement is not controlled, the grid cells at the purposely understocked and rotationally grazed research farm (Gellap Ost) are alternately treated by 'no grazing' and 'understocked grazing'. Within each time step (1 year), the landscape model calculates the following modules in the given order: water availability, vegetation dynamics and productivity (Figure 2). Each model is explained below.

2.3. Model Initialization

[13] Calculation of the slope (s) of each 1 ha cell is based on elevation (e_c) and side length (l = 100 m) of the respective cell and elevation of the neighboring cells (e_{nc})

$$s = \frac{e_C - e_{nc}}{l}. \quad (1)$$

Elevation was initialized with a digital elevation model (DEM), derived by remote sensing based radar data. The raster DEM is processed interferometrically from SRTM C Band data [*Jensen*, 2000] with an original spatial resolution of 88 m × 88 m in x and y direction and 1 m resolution of the altitude (z direction). The data have been preprocessed, applying a 3 × 3 kernel low-pass filter to reduce radar system inherent errors, caused by signal noise ("salt and pepper effect"), and shadow effects [*Lewis*, 1976]. Application of this filter leads to a smoothing of high contrast image areas. To fit the 100 × 100 m cell size of the landscape model, the DEM subset of the study area has been resampled, using a Nearest Neighbor algorithm.

[14] For initialization of the vegetation, we used the vegetation structure of an undisturbed dwarf shrub savannah. Since little is known about this vegetation structure we assumed an undisturbed coexistence of perennial grasses and woody vegetation. Thus initial vegetation condition for each cell was set to state 3 (compare Table 1).

2.4. Vegetation Dynamics

[15] We used a state and transition approach to simulate the vegetation dynamics. Transition probabilities between the vegetation states were calculated as Markovian stochastic processes [*Markov*, 1907]: a state at time t depends on the state at time $t - 1$ and the impact of the exogenous factors water availability, slope and present land use. A $m \times m$ transition matrix (P) contains the conditional probabilities p_{ij} that a cell in state i at time t will transition to state j at time $t + 1$. P is row standardized, such that the sum of transition probabilities from a given state is always equal to one. We derived transition probabilities by calculating transition probabilities of the process-based small-scale simulation model. To gain these values we ran the small-scale model for 100 years with 500 repetitions.

Table 1. Definition of Vegetation States for the Research Area[a]

	$Cover_{PG}$ (%)	$Cover_{W}$ (%)
State 1	30 – 100	40 – 100
State 2	0 – 29	40 – 100
State 3	50 – 100	0 – 40
State 4	10 – 49	0 – 40
State 5	0 – 9	10 – 40
State 6	0 – 9	0 – 9

[a]Columns refer to cover of the respective vegetation type (PG is perennial grass and W is woody vegetation). Rows refer to vegetation state, enumerated by 1–6.

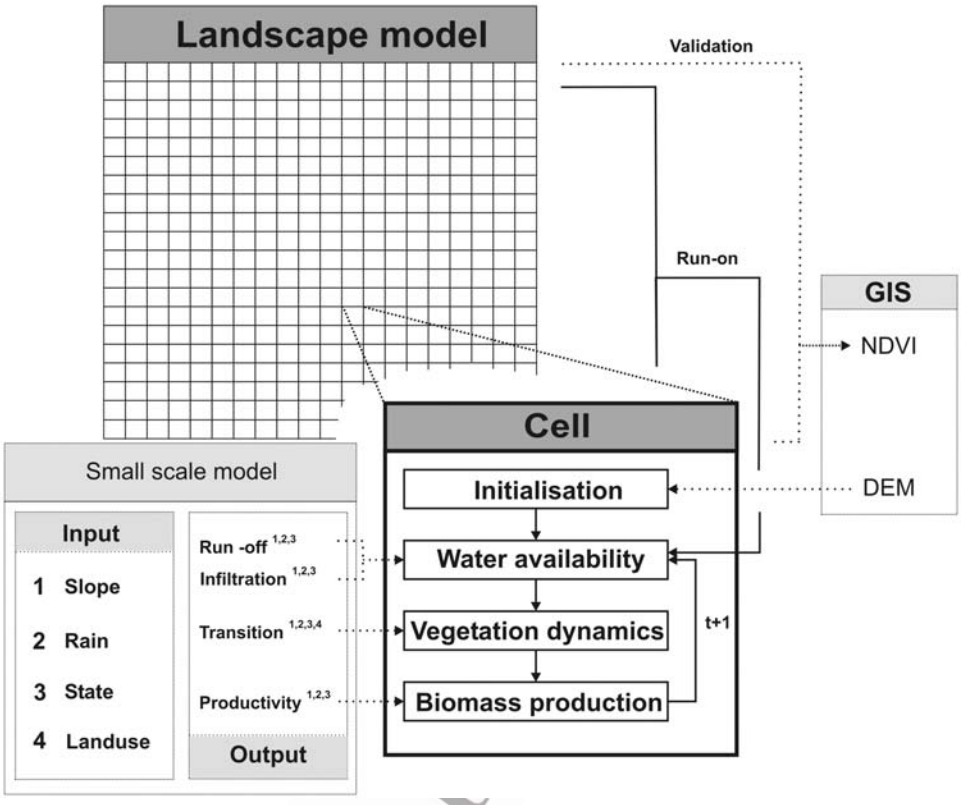

Figure 2. Visualization of mechanistic upscaling approach and simplified flowchart. We used a small-scale simulation model to derive data for vegetation dynamics, productivity, and linked hydrological processes of the landscape model. Elevation of the landscape's grid cells is initialized by remotely sensed digital elevation models (DEM). For validation, simulated annual biomass production is compared with remotely sensed estimates of annual biomass production (normalized differential vegetation index (NDVI)). Solid lines represent processes within the landscape model (flowchart). Dotted lines illustrate data flow between different disciplines and scales. Numbers refer to basic attributes of the small-scale model (input) affecting transferred data for the landscape model (output).

[16] Generally, we assume that (1) transition probabilities are constant over time and (2) transitions are spatially independent. An approach to model nonstationarity (i.e., variability in space and time of transition probabilities) is to switch between different stationary matrices [*Rejmanek et al.*, 1987]. To consider variability in space and time of transition probabilities related to water availability, slope, and land use option, we generated transition matrices for all combinations of these exogenous factors.

2.5. Productivity

[17] Annual phytomass production of the four vegetation types is dependent on the cells slope, present vegetation state, and water availability. For each vegetation type we calculated productivity coefficients from multiple linear regressions of biomass on slope, vegetation state and water availability simulated by the small scale model.

2.6. Water Availability

[18] We implemented two versions of the landscape model. One version disregards lateral exchange of surface water, while the other explicitly considers overland flow. In the first version, water availability (W_C) is dependent on annual precipitation (p_C). In the case of overland flow (second version), W_C is not only related to annual precipitation (p) but also to run-on (r_C) from neighboring cells and can be expressed by

$$W_c = p + r_c, \tag{2}$$

where p is homogeneous for all cells, whereas r_C is based on a cell specific capacity to absorb run-on (ir_C) and the contribution by run-off from neighboring cells (r_{NC})

$$r_C = r_{NC} - ir_C. \tag{3}$$

We used an iterative algorithm to calculate surface water flow for each simulated year: in the first step, each cell's $ir_{C,0}$ and $r_{NC,0}$, calculated by the small-scale model, are based on rain class as well as a cell's slope class and current vegetation state.

[19] In each following iterative step $r_{NC,i}$ is updated until infiltration of a cell is saturated ($ir_{C,i} = 0$) and until no more cells pass flow ($r_{NC,i} = 0$). For the next iterative step $ir_{C,i+1}$ is actualized by

$$ir_{C,i+1} = ir_{C,i} - r_{C,i}. \tag{4}$$

We used multiple flow direction methods to estimate surface water flow directions across cells [*Quinn et al.*, 1991; *Tarboton*, 1997]. Thus, cells with run-off allocate water fractionally to each lower neighbor cell in proportion to the respective slope.

2.7. Small-Scale Simulation Model

[20] Transition probabilities and phytomass production are derived from a small-scale simulation model [*Popp et al.*, 2009]. The spatially explicit and individual based model simulates the vegetation dynamics of a 1 ha area (100 × 100 m, 33 × 33 cells). Cell size is 3 m × 3 m, which corresponds to the maximum observed diameter of a shrub. Herbaceous vegetation (perennial grass and annuals) are treated as matrix plants, and a cell is either occupied or not. Woody plants are simulated individually and each cell contains a list of woody plant individuals. Slope angle is included by decreasing elevation values of the cells toward one side of the landscape. For each cell, water availability, establishment, aboveground biomass production, grazing and mortality are simulated in annual time steps.

2.7.1. Water Availability

[21] Cell-specific water availability in the various vegetation types is influenced by rainfall, run-off, run-on, evapotranspiration and competition. Surface run-off in semiarid and arid regions occurs primarily as infiltration excess overland flow from higher to lower areas controlled by infiltration characteristics of the soil surface rather than the storage capacity of the soil [*Wilcox et al.*, 2003]. Therefore, infiltration rates are related to the cell's soil texture [*Bergkamp*, 1998], vegetation cover [*Puigdefabregas*, 2005] and slope [*Chaplot and Le Bissonnais*, 2000]. Surface run-off occurring at cells with lowest elevation values at the edge of the simulated landscape leaves the system. Moreover, soil texture and vegetation cover have an impact on evaporation [*LeHouerou*, 1984; *Snyman*, 2000], reducing soil water content in the upper soil layer. Competitive effects of vegetation (i.e., vegetation-specific transpiration) reduce the water availability for establishment and, in cells with overlapping root systems, vegetation has a competitive effect on the neighboring vegetation types [*Callaway and Walker*, 1997]. To simplify the hydrological processes in our modeling approach we assume that all infiltrated water is evaporated or transpirated.

2.7.2. Establishment

[22] In arid and semiarid environments, sufficient moisture [*O'Connor*, 1994] and the availability of seeds [*O'Connor and Pickett*, 1992] are the main conditions for successful plant establishment. Furthermore, limited food for livestock increases the probability that livestock will feed on seedlings [*Carrick*, 2003]. Therefore, the cells' probability of successful establishment of perennial vegetation (woody plants and perennial grasses) is determined by site-specific probabilities of seed and water availability, as well as the probability to survive grazing. Annuals, producing large numbers of seeds and persistent seed banks [*Veenendaal et al.*, 1996] are only restricted by water availability and grazing pressure.

2.7.3. Growth

[23] Biomass production of the herbaceous vegetation is related to annual water availability for the two matrix plant types: annual and perennial grasses. For both vegetation types, we use a growth coefficient derived from rainfall-grass production relationships of various southern African savannah regions [*Higgins et al.*, 2000]. In contrast, annual biomass production of woody plant individuals depends on the impacts of water availability and is related to current height performance.

2.7.4. Grazing

[24] The model simulates grazing and browsing on herbaceous and woody vegetation. Vegetation types differ in their palatability for grazers and browsers. What and to which amount a plant's biomass will be consumed depends on its specific palatability as well as the relation of available biomass in the landscape and that necessary for forage.

2.7.5. Mortality

[25] Survival of perennial plants is environmentally determined by the availability of water and the impact of grazing by livestock [*Milton and Dean*, 2000]. We related the survival probability to these factors (water and grazing), since disturbances such as drought or overgrazing strongly influence productivity. Within the group of perennial plants, differences among species in disturbance tolerance are associated with physiological adaptations to disturbance.

2.8. Simulation Analysis

[26] We used the landscape model to simulate vegetation dynamics and productivity of perennial grass, annuals, dwarf shrubs and shrubs for 150 years. Effects of connectivity and spatial explicitness of overland flow on dynamics and productivity of the most abundant vegetation types was assessed for a purposely understocked and rotationally grazed research farm (Gellap Ost) (0.05 SSU ha^{-1}) and a communal and overstocked range land (Nabaos) (0.2 SSU ha^{-1}). For model analysis, we used the years 1985 to 2000, as remotely sensed data is available only for this time period, and initialization effects could be excluded. Due to the stochastic processes in the model, no single run is representative. Therefore, we initiated 50 repeats for each model type and scenario.

2.9. Model Validation

[27] We compared simulation results of annual phytomass production for both study sites (low grazing impact versus high grazing impact) with remotely sensed Normalized Difference Vegetation Index (NDVI) as an indicator for interannual variability. Because NDVI indicates relative values we also compared our model results with field data on biomass production and cover for perennial grasses.

[28] Remotely sensed NDVI is strongly correlated with phytomass production [e.g., *Tucker et al.*, 1986; *Prince and Goward*, 1996; *Yang and Prince*, 2000; *Wessels et al.*, 2006]. NDVI is calculated from the red and near-infrared channels from multispectral remote sensing imagery [*Tucker and Choudhury*, 1987]

$$NDVI = \frac{NIR - R}{NIR + R}, \tag{5}$$

where NIR is the reflectance in the near infrared band (0,72 – 1,10 μm) and R the reflectance in the red band (0,58–0,68 μm). NDVI time series data for 1985 to 2001 were obtained from NOAA/NASA Pathfinder Land data archive (PAL). However, due to the failure of NOAA-11, no

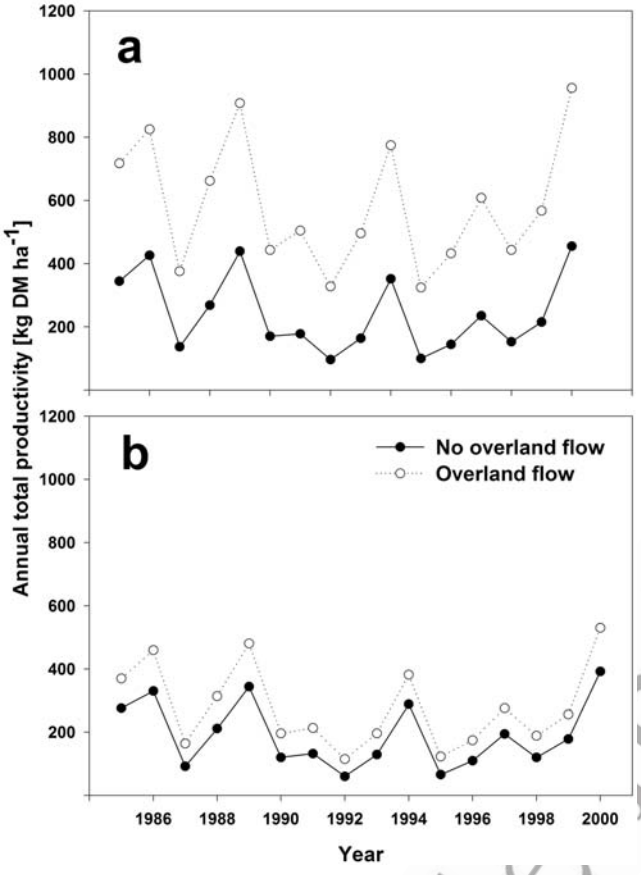

Figure 3. Time series of annual total productivity. Medians of 500 simulation replicates are shown. Annual total productivity at (a) low grazing intensity (Gellap) is strongly affected by overland flow. Low impact of overland flow can be found at the scenario with (b) high grazing intensity (Nabaos). Black circles represent scenarios without overland flow, and white circles represent scenarios with overland flow.

NDVI data were available between July and December 1994 (http://www2.ncdc.noaa.gov/docs/gviug/html/c2/sec2−0.htm).

[29] We have used the seasonal integral or accumulated NDVI (I-NDVI) that was calculated for each sampling domain from seasonal summations (October to September) of differences between NDVI and minimum NDVI from the seasons 1985−1986 to 2000−2001 [*Holm et al.*, 2003]. Reference values of NDVI have been calculated for both study sites over an area of 8 km^2 each.

3. Results

3.1. Annual Total Phytomass

[30] Annual total phytomass simulated by the model without overland flow ranged from 475 t per ha at the scenario with low grazing intensity (Gellap Ost, Figure 3a) in 2000 to 79 t per ha at the scenario with high grazing intensity (Nabaos, Figure 3b) in 1992. In contrast, in all simulations using the model including overland flow, annual total phytomass ranged from 983 t per ha at low grazing intensity in 2000 (Figure 3a) to 112 t per ha at high grazing intensity in 1992 (Figure 3b).

[31] Averaged over a period of 15 years in the model without overland flow, total phytomass production simulated by the scenario with low grazing intensity exceeds total phytomass production simulated by the scenario with high grazing intensity 1.32-fold. In the model including overland flow, the 15 year average of total phytomass production for low grazing intensity exceeds the total phytomass production for the high grazing intensity scenario 2.24-fold.

[32] Linear regression analysis for the model without overland flow indicated that total phytomass at the scenario with low grazing intensity ($R^2 = 0.97$, $p < 0.001$) and the scenario with high grazing intensity ($R^2 = 0.99$, $p < 0.001$) increased with annual precipitation. In the model that includes overland flow, total phytomass equally increased with annual precipitation for the scenario with low grazing intensity and for high grazing intensity (both $R^2 = 0.98$, $p < 0.001$). In the model that includes overland flow, total phytomass production is 2.61-fold higher at the scenario with low grazing intensity and 1.54-fold higher at the scenario with high grazing intensity, than that of the model without overland flow.

3.2. Productivity of Vegetation Types

[33] In the model without overland flow, productivity of annuals contributed 45% to the mean total productivity, followed by perennial grass (31%), shrubs (18%) and dwarf shrubs (6%) for the scenario with low grazing intensity (Figure 4a). At the scenario with high grazing intensity (Figure 4c), the proportion in mean annual total productivity was clearly decreased for perennial grasses (19%) and dwarf shrubs (3%), and dominance was shifted toward annuals (57%) and shrubs (22%).

[34] In the model that includes overland flow, it is not only total annual phytomass production that is affected by spatial exchange of surface water, precipitation and land use; it is also productivity of the four most abundant vegetation types (perennial grass, annuals, dwarf shrubs and shrubs). Including overland flow in simulating dynamics and productivity of these vegetation types has the strongest impact at the scenario with low grazing intensity (Figure 4b): perennial grass contributes with 47% most to the mean total productivity, followed by annuals (28%), shrubs (19%) and dwarf shrubs (6%). At the scenario with high grazing intensity (Figure 4d), no effect of overland flow on the proportion of vegetation types in mean total productivity could be identified. However, the model excluding overland flow clearly indicates a decrease in the proportion in mean annual total productivity for perennial grasses (19%) and dwarf shrubs (3%), and dominance was shifted toward annuals (60%) and shrubs (18%).

3.3. Disturbance and Overland Flow

[35] Disturbance in the form of overgrazing can have a strong impact on lateral exchange of surface water (Figure 5). Light grazing intensities lead to 83% of run-on cells in the total number of cells (% of area) as well as high mean run-on in these cells (85%) for the years 1985 to 2000. In contrast, the proportion of run-on cells to total area decreases to 63% with low mean run-on of 40% at the scenario with high grazing intensity.

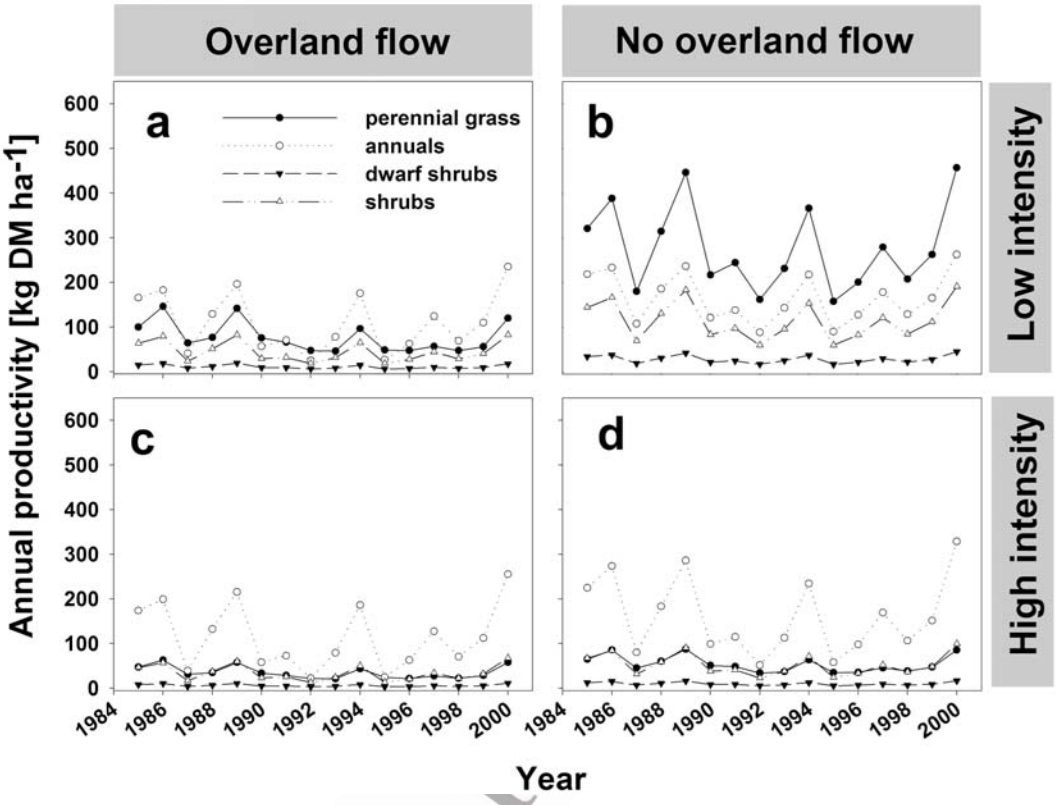

Figure 4. Time series of annual productivity for the simulated vegetation types. Medians of 500 simulation replicates are shown. Different management scenarios ((a and c) Gellap and (b and d) Nabaos) are shown. Figures 4a and 4b show results for simulation models without overland flow, and Figures 4c and 4d refer to simulation models including overland flow. Black circles refer to perennial grass, white circles refer to annual forbs, black triangles refer to dwarf shrubs, and white triangles refer to shrubs.

3.4. Validation of Simulated Phytomass Production

3.4.1. Estimated I-NDVI

[36] Vegetation at the communal rangelands (Nabaos) had lower I-NDVI than vegetation at the research farm (Gellap Ost) across all growth seasons (Figure 6). The lowest value of 0.5 at the communal rangelands in 1987 contrasts with the highest value of 1.6 at the research farm in 2000. Averaged over the time span of 15 years, I-NDVI measured at the research farm exceeds I-NDVI measured at the communal rangelands 1.27-fold. Linear regression analysis indicated that I-NDVI is correlated with annual precipitation at the research farm ($R^2 = 0.81$, $p < 0.001$) and the communal rangelands ($R^2 = 0.91$, $p < 0.001$).

3.4.2. Comparison of Simulated Phytomass and Estimated I-NDVI

[37] We compared simulated total annual phytomass with remotely sensed estimates of annual phytomass production (I-NDVI) to test if the landscape model displays vegetation dynamics in a simplified but realistic way. The linear regression relationship between simulated total phytomass and I-NDVI (Figure 7) accounted for little more variance at the model with overland flow ($R^2 = 0.79$, $p < 0.001$) than for the model version without overland flow ($R^2 = 0.69$, $p < 0.001$). However, the slopes of the linear regression relationship indicate that total productivity simulated by the model with overland flow ($y = -308 + x * 978$) exceeds

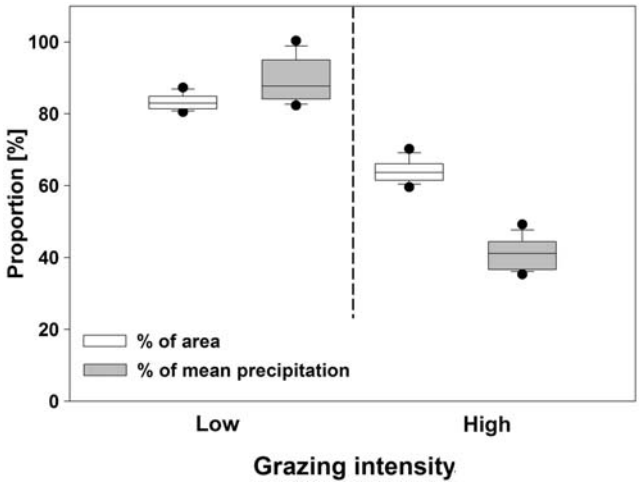

Figure 5. Importance of overland flow under different grazing intensities. At the scenario with low grazing intensity (left side) overland flow leads to high proportion of run-on cells to total area (white box plots) and high values of mean run-on (gray box plots). Mean run-on is given as a percent in total annual rain. In contrast, proportion of run-on cells as well as mean proportion of run-on at the scenario with high grazing intensity (right side) display low values.

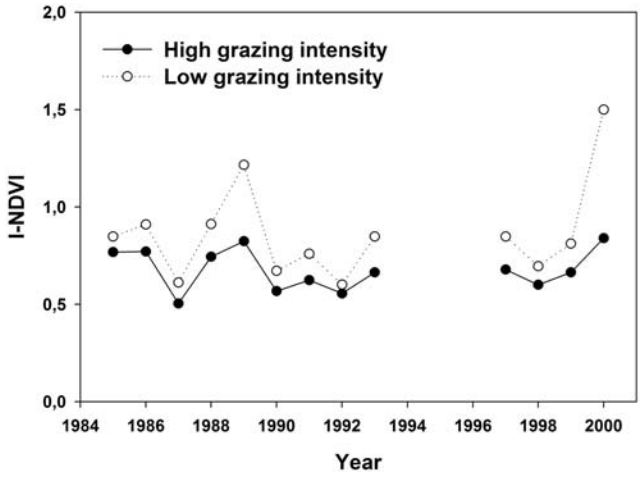

Figure 6. Time series of integrated normalized differential vegetation index (I-NDVI). I-NDVI was calculated for each sampling domain from seasonal summations (October–September) of differences between NDVI and minimum NDVI from the seasons 1985–1986 to 2000–2001. Black circles represent the scenario with low grazing intensity (Gellap), and white circles represent the scenario with high grazing intensity (Nabaos).

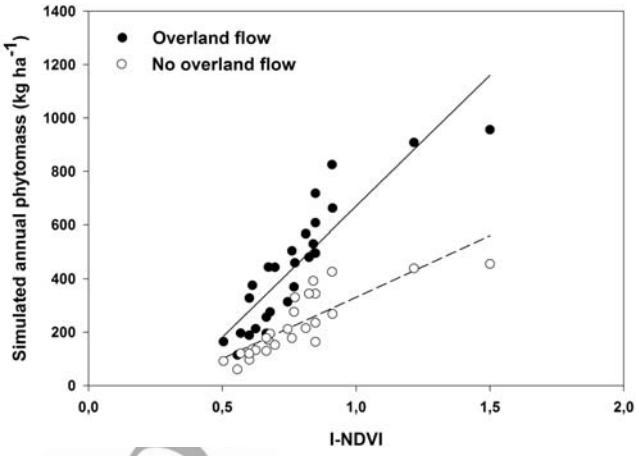

Figure 7. Comparison of simulated phytomass and measured I-NDVI. For both simulation methods and both management methods modeled total phytomass in each year from 1985 to 2000 were compared with remotely sensed indices of phytomass (I-NDVI). I-NDVI images cover 8km^2 of both the research farm with low grazing intensity (Gellap) and communal rangeland with high grazing intensity (Nabaos).

productivity simulated by the model without overland flow ($y = -129 + x * 460$).

3.4.3. Comparison of Simulated Phytomass and Cover With Measured Field Data

[38] Perennial grass cover and biomass production simulated by the model with overland flow for the year 2001 matched the field observations [*Prinsloo and Bester*, 2003; *Wolkenhauer*, 2004] more effectively than simulation results from the model version without overland flow (Table 2).

4. Discussion

[39] The aim of our study was to present a method to transfer and integrate existing information on vegetation dynamics and hydrological processes between spatial scales. Combining technologies of remote sensing technology and stochastic modeling, we are able to successful extrapolate vegetation dynamics, composition and productivity to an order of magnitude one hundred times greater than the original scale. Using a small-scaled simulation model, the influence of exogenous and endogenous variables (vegetation state, precipitation, management and topography) on transition probabilities and phytomass production were estimated.

[40] In the past, transition probabilities of stochastic landscape models were mainly estimated by using data from observations, and measured from empirical studies, aerial photography and satellite images [e.g., *Muller and Middleton*, 1994; *Brown et al.*, 2000; *Jenerette and Wu*, 2001; *Weng*, 2002]. Uncertainty in these studies remained relatively high because data was limited, i.e., transition probabilities were derived from short-term data [*Baker*, 1989]. The few studies that use a fine-scale model to drive a landscape model [e.g., *Acevedo et al.*, 1995] did not include microscale processes like ecohydrological feedback mechanisms and spatial exchange like surface water flow.

[41] The simulation results of our landscape model show that the explicit consideration of surface water flow can have a strong impact on vegetation dynamics, composition and productivity at the landscape scale. At low grazing intensity, a high number of run-on cells with high infiltration capacities serve as sinks for input by surface water flow. Spatial exchange of surface water among vegetation patches increases biomass production when compared to simulations where overland flow was not considered. In contrast, disturbance in the form of overgrazing reduces positive feedbacks through vegetation and hydrology and therefore decreases infiltration capacity of potential run-on cells. The buffer capacity of these hydrological sinks is reduced, run-off increases and biomass production remains low. The consideration of overland flow causes water to flow downstream out of the simulated system and artificial droughts can occur even in years with good precipitation.

[42] This general process has been observed in other semiarid and arid areas where the spatial exchange between patches of vegetation affects the resilience of ecosystems [*van de Koppel and Rietkerk*, 2004; *Ludwig et al.*, 2005]. Ecosystems heterogeneous in space and linked by spatial feedback mechanisms provide potential for buffering positive feedback. Coarse-scale catastrophic shifts are more likely in systems that have little spatial heterogeneity or

Table 2. Comparison of Model Output With Field Data on Percentage Coverage and Biomass Production of Perennial Grasses for the Research Area With High and Low Grazing Pressure[a]

	Field Data	Overland Flow	No Overland Flow
Cov_L (%)	50	44 (2.2)	12 (0.9)
Cov_H (%)	1	6 (1.0)	5 (0.6)
$Prod_L$ (t dry matter/ha)	258	262 (5.6)	48 (3.1)

[a]Here Cov is coverage and Prod is biomass production, and H is high and L is low grazing pressure. Standard deviations for the model output are given in the parentheses.

no spatial feedback mechanisms to compensate for positive feedback. Taking these conclusions into account, our model results provide additional insights into the impact of spatial exchange of water on ecosystem service and the functioning of arid rangelands. Overland flow not only decreases total annual productivity but also affects vegetation composition. At low grazing intensities, the explicit consideration of overland flow favors high abundance of vegetation states with high cover of perennial grasses, whereas vegetation states with annual vegetation were frequent where overland flow was excluded. In contrast, only low effects of overland flow on vegetation composition could be observed at high grazing intensities (Nabaos). Here, vegetation states consist mainly of bare ground, shrubs and, in years of high precipitation, annuals, which dominate the simulated landscape at both model versions. Although our results demonstrate the high relevance of the explicit inclusion of overland flow at landscape scale for vegetation dynamics, until now it has seldom been recognized, quantified and incorporated into management decisions [*Rastetter et al.*, 2003; *van de Koppel and Rietkerk*, 2004].

[43] Generally, rotational grazing strategies have been proposed to increase stocking capacity, improve animal gains, and improve forage production and range condition [e.g., *Fynn and O'Connor*, 2000]. In this paper, we have demonstrated that in semiarid and arid rangelands with distinct topography, the rotation of livestock between different paddocks combined with moderate stocking rates becomes even more important, as nondegraded paddocks serve as hydrological sinks which catch and conserve surface run-off from degraded paddocks with low vegetation cover. A thorough understanding of overland flow is an important precondition for improving the management of semiarid and arid rangelands with distinct topography.

[44] **Acknowledgments.** We gratefully acknowledge support from the German Ministry of Education and Research (BMBF) through the framework of BIOTA southern Africa (01LC0024A) and the German BMBF project "Preis des Wassers." Furthermore we are grateful to our CSIR colleague Russell Main who invested his time in making our German-English less painful for the native English audience.

References

Acevedo, M. F., D. L. Urban, and M. Ablan (1995), Transition and gap models of forest dynamics, *Ecol. Appl.*, *5*, 1040–1055, doi:10.2307/2269353.

Baker, W. L. (1989), A review of models of landscape change, *Landscape Ecol.*, *2*, 111–133, doi:10.1007/BF00137155.

Balzter, H. (2000), Markov chain models for vegetation dynamics, *Ecol. Modell.*, *126*, 139–154, doi:10.1016/S0304-3800(00)00262-3.

Bergkamp, G. (1998), A hierarchical view of the interactions of runoff and infiltration with vegetation and microtopography in semiarid shrublands, *Catena*, *33*, 201–220.

Brown, D. G., B. C. Pijanowski, and J. D. Duh (2000), Modeling the relationships between land use and land cover on private lands in the upper midwest, USA, *J. Environ. Manage.*, *59*, 247–263, doi:10.1006/jema.2000.0369.

Callaway, R. M., and L. R. Walker (1997), Competition and facilitation: A synthetic approach to interactions in plant communities, *Ecology*, *78*, 1958–1965.

Carrick, P. J. (2003), Competitive and facilitative relationships among three shrub species, and the role of browsing intensity and rooting depth in the Succulent Karoo, South Africa, *J. Veg. Sci.*, *14*, 761–772.

Chaplot, V., and Y. Le Bissonnais (2000), Field measurements of interrill erosion under different slopes and plot sizes, *Earth Surf. Processes Landforms*, *25*, 145–153.

Crockford, R. H., and D. P. Richardson (2000), Partitioning of rainfall into throughfall, stemflow, and interception: Effect of forest type, ground cover and climate, *Hydrol. Processes*, *14*, 2903–2920.

Fynn, R. W. S., and T. G. O'Connor (2000), Effect of stocking rate and rainfall on rangeland dynamics and cattle performance in a semi-arid savanna, South Africa, *J. Appl. Ecol.*, *37*, 491–507.

Heuvelink, G. B. M. (1998), Uncertainty analysis in environmental modelling under a change of spatial scale, *Nutr. Cycling Agroecosyst.*, *50*, 255–264, doi:10.1023/A:1009700614041.

Higgins, S. I., W. J. Bond, and W. S. W. Trollope (2000), Fire, resprouting and variability: A recipe for grass-tree coexistence in savanna, *J. Ecol.*, *88*, 213–229, doi:10.1046/j.1365-2745.2000.00435.x.

Holm, A. M., S. W. Cridland, and M. L. Roderick (2003), The use of time-integrated NOAA NDVI data and rainfall to assess landscape degradation in the arid shrubland of western Australia, *Remote Sens. Environ.*, *85*, 145–158, doi:10.1016/S0034-4257(02)00199-2.

Huxman, T. E., B. P. Wilcox, D. D. Breshears, R. L. Scott, K. A. Snyder, E. E. Small, K. Hultine, W. T. Pockman, and R. B. Jackson (2005), Ecohydrological implications of woody plant encroachment, *Ecology*, *86*, 308–319.

Jenerette, G. D., and J. G. Wu (2001), Analysis and simulation of land-use change in the central Arizona–Phoenix region, USA, *Landscape Ecol.*, *16*, 611–626, doi:10.1023/A:1013170528551.

Jensen, J. R. (2000), *Remote Sensing of Environment: An Earth Resource Perspective*, Prentice Hall, Upper Saddle River, N. J.

Kuiper, S. M., and M. E. Meadows (2002), Sustainability of livestock farming in the communal lands of southern Namibia, *Land Degrad. Dev.*, *13*, 1–15, doi:10.1002/ldr.476.

LeHouerou, H. N. (1984), Rain use efficiency: A unifying concept in arid-land ecology, *J. Arid Environ.*, *7*, 213–247.

Levin, S. A. (1992), The problem of pattern and scale in ecology, *Ecology*, *73*, 1943–1967, doi:10.2307/1941447.

Lewis, A. J. (Ed.) (1976), *Geoscience Applications of Imaging Radar Systems, Remote Sensing of the Electromagnetic Spectrum, Remote Sensing Commission of Association of American Geographers*, vol. 3, Assoc. of Am. Geogr., Washington, D. C.

Logofet, D. O., and E. V. Lesnaya (2000), The mathematics of Markov models: What Markov chains can really predict in forest successions, *Ecol. Modell.*, *126*, 285–298, doi:10.1016/S0304-3800(00)00269-6.

Ludwig, J. A., B. P. Wilcox, D. D. Breshears, D. J. Tongway, and A. C. Imeson (2005), Vegetation patches and runoff-erosion as interacting ecohydrological processes in semiarid landscapes, *Ecology*, *86*, 288–297, doi:10.1890/03-0569.

Markov, A. (1907), Extension of the limit theorems of probability theory to the sum of variables connected in a chain, *Notes Imp. Acad. Sci. St. Petersburg*, *22*, 61–80.

Miller, J. R., M. G. Turner, E. A. H. Smithwick, C. L. Dent, and E. H. Stanley (2004), Spatial extrapolation: The science of predicting ecological patterns and processes, *BioScience*, *54*, 310–320, doi:10.1641/0006-3568(2004)054[0310:SETSOP]2.0.CO;2.

Milton, S. J., and W. R. J. Dean (2000), Disturbance, drought and dynamics of desert dune grassland, South Africa, *Plant Ecol.*, *150*, 37–51, doi:10.1023/A:1026585211708.

Muller, M. R., and J. Middleton (1994), A Markov model of land-use change dynamics in the Niagara region, Ontario, Canada, *Landscape Ecol.*, *9*, 151–157.

Noy-Meir, I. (1973), Desert ecosystems: Environment and producers, *Annu. Rev. Ecol. Syst.*, *4*, 25–52, doi:10.1146/annurev.es.04.110173.000325.

O'Connor, T. G. (1994), Composition and population responses of an African savanna grassland to rainfall and grazing, *J. Appl. Ecol.*, *31*, 155–171, doi:10.2307/2404608.

O'Connor, T. G., and G. A. Pickett (1992), The influence of grazing on seed production and seed banks of some African savanna grasslands, *J. Appl. Ecol.*, *29*, 247–260.

Peters, A. J., M. D. Eve, E. H. Holt, and W. G. Whitford (1997), Analysis of desert plant community growth patterns with high temporal resolution satellite spectra, *J. Appl. Ecol.*, *34*, 418–432, doi:10.2307/2404887.

Peters, D. P. C., and K. M. Havstad (2006), Nonlinear dynamics in arid and semi-arid systems: Interactions among drivers and processes across scales, *J. Arid Environ.*, *65*, 196–206, doi:10.1016/j.jaridenv.2005.05.010.

Popp, A., N. Blaum, and F. Jeltsch (2009), Ecohydrological feedback mechanisms in arid rangelands: Simulating the impacts of topography and land use, *Basic Appl. Ecol.*, *10*, 319–329, doi:10.1016/j.baae.2008.06.002.

Prince, S. D., and S. N. Goward (1996), Evaluation of the NOAA/NASA Pathfinder AVHRR land data set for global primary production modelling, *Int. J. Remote Sens.*, *17*, 217–221, doi:10.1080/01431169608948999.

Prinsloo, R., and F. V. Bester (2003), Determination of grazing capacities in the southern regions of Namibia using the grazing index method, paper presented at Reporting Conference, Minist. of Agric., Windhoek, Namibia.

Puigdefabregas, J. (2005), The role of vegetation patterns in structuring runoff and sediment fluxes in drylands, *Earth Surf. Processes Landforms*, *30*, 133–147, doi:10.1002/esp.1181.

Quinn, P., K. Beven, P. Chevallier, and O. Planchon (1991), The prediction of hillslope flow paths for distributed hydrological modeling using digital terrain models, *Hydrol. Processes*, *5*, 59–79, doi:10.1002/hyp.3360050106.

Rango, A., S. L. Tartowski, A. Laliberte, J. Wainwright, and A. Parsons (2006), Islands of hydrologically enhanced biotic productivity in natural and managed arid ecosystems, *J. Arid Environ.*, *65*, 235–252, doi:10.1016/j.jaridenv.2005.09.002.

Rastetter, E. B., J. D. Aber, D. P. C. Peters, D. S. Ojima, and I. C. Burke (2003), Using mechanistic models to scale ecological processes across space and time, *BioScience*, *53*, 68–76, doi:10.1641/0006-3568(2003)053[0068:UMMTSE]2.0.CO;2.

Reid, W. V. (2005), *Ecosystems and Human Well-Being: Wetlands and Water Synthesis: A Report of the Millennium Ecosystem Assessment*, 1–137 pp., World Resour. Inst., Washington, D. C.

Rejmanek, M., C. E. Sasser, and J. G. Gosselink (1987), Modeling of vegetation dynamics in the Mississippi river deltaic plain, *Vegetatio*, *69*, 133–140, doi:10.1007/BF00038694.

Scheffer, M., S. Carpenter, J. A. Foley, C. Folke, and B. Walker (2001), Catastrophic shifts in ecosystems, *Nature*, *413*, 591–596, doi:10.1038/35098000.

Seyfried, M. S., S. Schwinning, M. A. Walvoord, W. T. Pockman, B. D. Newman, R. B. Jackson, and F. M. Phillips (2005), Ecohydrological control of deep drainage in arid and semiarid regions, *Ecology*, *86*, 277–287.

Snyman, H. A. (2000), Soil-water utilisation and sustainability in a semi-arid grassland, *Water SA*, *26*, 333–341.

Strayer, D. L., H. A. Ewing, and S. Bigelow (2003), What kind of spatial and temporal details are required in models of heterogeneous systems?, *Oikos*, *102*, 654–662, doi:10.1034/j.1600-0706.2003.12184.x.

Tarboton, D. G. (1997), A new method for the determination of flow directions and upslope areas in grid digital elevation models, *Water Resour. Res.*, *33*, 309–319, doi:10.1029/96WR03137.

Tongway, D. J., and J. A. Ludwig (1997), The conservation of water and nutrients within landscapes, in *Landscape Ecology, Function and Management: Principles from Australia's Rangelands*, edited by J. A. Ludwig et al., pp. 13–22, Commonw. Sci. and Ind. Res. Organ., Melbourne, Victoria, Australia.

Tucker, C. J., and B. J. Choudhury (1987), Satellite remote-sensing of drought conditions, *Remote Sens. Environ.*, *23*, 243–251, doi:10.1016/0034-4257(87)90040-X.

Tucker, C. J., C. O. Justice, and S. D. Prince (1986), Monitoring the grasslands of the Sahel 1984–1985, *Int. J. Remote Sens.*, *7*, 1571–1581, doi:10.1080/01431168608948954.

Turner, M. G. (1989), Landscape ecology: The effect of pattern on process, *Annu. Rev. Ecol. Syst.*, *20*, 171–197, doi:10.1146/annurev.es.20.110189.001131.

Urban, D. L. (2005), Modeling ecological processes across scales, *Ecology*, *86*, 1996–2006, doi:10.1890/04-0918.

van de Koppel, J., and M. Rietkerk (2004), Spatial interactions and resilience in arid ecosystems, *Am. Nat.*, *163*, 113–121, doi:10.1086/380571.

van de Koppel, J., et al. (2002), Spatial heterogeneity and irreversible vegetation change in semiarid grazing systems, *Am. Nat.*, *159*, 209–218, doi:10.1086/324791.

Veenendaal, E. M., W. H. O. Ernst, and G. S. Modise (1996), Effect of seasonal rainfall pattern on seedling emergence and establishment of grasses in a savanna in south-eastern Botswana, *J. Arid Environ.*, *32*, 305–317.

Walvoord, M. A., M. A. Plummer, F. M. Phillips, and A. V. Wolfsberg (2002), Deep arid system hydrodynamics: 1. Equilibrium state and response times in thick desert vadose zones, *Water Resour. Res.*, *38*(12), 1308, doi:10.1029/2001WR000824.

Weaver, K., and A. H. Perera (2004), Modelling land cover transitions: A solution to the problem of spatial dependence in data, *Landscape Ecol.*, *19*, 273–289, doi:10.1023/B:LAND.0000030418.90245.4b.

Weng, Q. H. (2002), Land use change analysis in the Zhujiang delta of China using satellite remote sensing, GIS and stochastic modelling, *J. Environ. Manage.*, *64*, 273–284, doi:10.1006/jema.2001.0509.

Wessels, K. J., S. D. Prince, N. Zambatis, S. Macfadyen, P. E. Frost, and D. Van Zyl (2006), Relationship between herbaceous biomass and 1-km^2 Advanced Very High Resolution Radiometer (AVHRR) NDVI in Kruger National Park, South Africa, *Int. J. Remote Sens.*, *27*, 951–973, doi:10.1080/01431160500169098.

Wessman, C. A. (1992), Spatial scales and global change: Bridging the gap from plots to GCM grid cells, *Annu. Rev. Ecol. Syst.*, *23*, 175–200, doi:10.1146/annurev.es.23.110192.001135.

Westoby, M., B. Walker, and I. Noymeir (1989), Opportunistic Management for rangelands not at equilibrium, *J. Range Manage.*, *42*, 266–274, doi:10.2307/3899492.

Wilcox, B. P., D. D. Breshears, and C. D. Allen (2003), Ecohydrology of a resource-conserving semiarid woodland: Effects of scale and disturbance, *Ecol. Monogr.*, *73*, 223–239, doi:10.1890/0012-9615(2003)073[0223:EOARSW]2.0.CO;2.

Winand Staring Centre (1991), *World Map of the Status of Human-Induced Soil Degradation*, 2nd ed., U. N. Environ. Prog., Nairobi.

Wolkenhauer, C. (2004), Vergleichende vegetationsökologische untersuchungen auf den farmgebieten Gellap-ost (rotationsweide) und Nabaos (kommunales weideland) im südlichen Namibia, M.Sc. thesis, University of Hamburg, Hamburg, Germany.

Wootton, J. T. (2001), Local interactions predict large-scale pattern in empirically derived cellular automata, *Nature*, *413*, 841–844, doi:10.1038/35101595.

Yang, J., and S. D. Prince (2000), Remote sensing of savanna vegetation changes in eastern Zambia 1972–1989, *Int. J. Remote Sens.*, *21*, 301–322, doi:10.1080/014311600210849.

Zika, M., and K. H. Erb (2009), The global loss of net primary production resulting from human-induced soil degradation in drylands, *Ecol. Econ.*, doi:10.1016/j.ecolecon.2009.06.014, in press.

N. Blaum and F. Jeltsch, Department of Plant Ecology and Nature Conservation, University of Potsdam, Maulbeerallee 3, D-14469 Potsdam, Germany.

A. Popp, Potsdam Institute for Climate Impact Research, Telegraphenberg, D-14473 Potsdam, Germany. (popp@pik-potsdam.de)

M. Vogel, Natural Resources and the Environment Division, Council for Scientific and Industrial Research, P.O. Box 395, Pretoria 0001, South Africa.